

Provided for non-commercial research and education use.
Not for reproduction, distribution or commercial use.



(This is a sample cover image for this issue. The actual cover is not yet available at this time.)

This article appeared in a journal published by Elsevier. The attached copy is furnished to the author for internal non-commercial research and education use, including for instruction at the authors institution and sharing with colleagues.

Other uses, including reproduction and distribution, or selling or licensing copies, or posting to personal, institutional or third party websites are prohibited.

In most cases authors are permitted to post their version of the article (e.g. in Word or Tex form) to their personal website or institutional repository. Authors requiring further information regarding Elsevier's archiving and manuscript policies are encouraged to visit:

<http://www.elsevier.com/copyright>



Contents lists available at SciVerse ScienceDirect

European Journal of Pharmaceutical Sciences

journal homepage: www.elsevier.com/locate/ejps

QSAR, docking and *in vitro* studies for anti-inflammatory activity of cleomiscosin A methyl ether derivatives

Shelly Sharma^a, Sunil Kumar Chattopadhyay^{a,*}, Dharmendra Kumar Yadav^b, Feroz Khan^b, Shilpa Mohanty^c, Anil Maurya^c, Dnyaneshwar Umrao Bawankule^c

^a Process Chemistry and Technology Department, CSIR–Central Institute of Medicinal and Aromatic Plants (CSIR–CIMAP), Lucknow 226 015, India

^b Metabolic and Structural Biology Department, CSIR–Central Institute of Medicinal and Aromatic Plants (CSIR–CIMAP), Lucknow 226 015, India

^c Molecular Bioprospection Division, CSIR–Central Institute of Medicinal and Aromatic Plants (CSIR–CIMAP), Lucknow 226 015, India

ARTICLE INFO

Article history:

Received 21 August 2012

Received in revised form 13 September 2012

Accepted 15 September 2012

Available online 25 September 2012

Keywords:

Cleomiscosin A methyl ether
Novel polyhalogenated derivative
Anti-inflammatory activity
QSAR

ABSTRACT

A series of five (**6a–8b**) novel polyhalogenated derivatives and an interesting ester (**9a**) derivative have been synthesized from cleomiscosin A methyl ether. All the six derivatives were subjected to *in silico* QSAR modeling and docking studies and later the predicted results were confirmed through *in vitro* experiments. QSAR modeling results showed that compounds **6a** and **9a** possessed anti-inflammatory activity comparable or even higher than diclofenac sodium. Docking results revealed that compounds **9a** and **6a** showed very good anti-inflammatory activity due to low docking energies of viz., IL6 (–92.45 and –81.993 kcal mol^{–1}), TNF- α (–94.992 and –69.235 kcal mol^{–1}) and IL1 β (–67.462 and –65.985 kcal mol^{–1}). Further all the six novel derivatives were subjected for *in vitro* anti-inflammatory activity using primary macrophages cell culture bioassay system. At the initial doses of 1 μ g/ml and 10 μ g/ml, the pro-inflammatory cytokines (IL-1 β , IL-6 and TNF- α) were quantified from cell culture supernatant using enzyme linked immunosorbent assay (ELISA). The *in vitro* effect of **6a–9a** on cell viability in mouse peritoneal macrophage cells isolated from mice was evaluated using MTT assay. The *in silico* and *in vitro* data suggested that all the derivatives might be considered as potential anti-inflammatory drug-like molecules.

© 2012 Elsevier B.V. All rights reserved.

1. Introduction

Inflammation is the body's immediate response to damage to its tissues and cells by pathogens, noxious stimuli such as chemicals, or physical injury. Acute inflammation is a short-term response that usually results in healing: leukocytes infiltrate the damaged region, removing the stimulus and repairing the tissue. Chronic inflammation, by contrast, is a prolonged, dysregulated and maladaptive response that involves active inflammation, tissue destruction and attempts at tissue repair. Such persistent inflammation is associated with many chronic human conditions and diseases, including allergy, atherosclerosis, cancer, arthritis and autoimmune diseases. To overcome the challenges of inflammatory disorders, several classes of anti-inflammatory drugs have been used. These include Non-steroidal anti-inflammatory drugs (NSAIDs), Immune Selective Anti-Inflammatory Derivatives (ImSAIDs), corticosteroids etc. The widespread use of NSAIDs in

the treatment of rheumatoid arthritis and osteoarthritis leads to adverse side effects like gastrointestinal ulceration, bleeding and platelet dysfunction. The long-term use of corticosteroids in rheumatoid arthritis increases the risk of serious side effects like Cushing's habitus, hypertension, hyperglycemia, muscular weakness, increased susceptibility to infection, osteoporosis, glaucoma, psychiatric disturbances, growth arrest, etc. (Gautam and Jachak, 2009).

A very large percentage of our population depends on these anti-inflammatory drugs in spite of their severe side effects. A logical alternate has to provide against these side effects causing drugs and therefore, natural products can only express a great hope in the identification of biologically active metabolites that can be obtained directly from the plant source or can be semi-synthetically derived which serves as an alternate approach towards anti-inflammatory drugs (Butler, 2008). A report on the origin of the drugs developed between 1981 and 2002 showed that natural products or natural product-derived drugs comprised 28% of all new chemical entities (NCEs) launched onto the market. In addition, 24% of these NCEs were synthetic or natural mimic compounds, based on the study of pharmacophores related to natural products. This combined percentage (52% of all NCEs) suggests that natural products are important sources for new drugs and are good

* Corresponding author. Address: Process Chemistry and Technology Department, Central Institute of Medicinal and Aromatic Plants, Council of Scientific & Industrial Research, P.O.–CIMAP, Kukrail Picnic Spot Road, Lucknow 226 015, UP, India. Tel.: +91 9648029167; fax: +91 522 2342666.

E-mail address: chattsk@yahoo.com (S.K. Chattopadhyay).

lead compounds suitable for further modification during the drug development process (Chin et al., 2006). The recent development in the field of science provides the *in vitro*, *in silico* screening of natural product derived chemical entities and the semi synthetic derivatives. This increased interest in the pharmaceutical industry as a productive and cost-effective technology for the search of novel hit or lead compounds.

Cleome viscosa (Family: Capparidaceae) commonly called as Wild mustard, Hur Hur (in Hindi) is distributed throughout the greater part of India, mostly in wastelands. In Ayurvedic system of medicine the plant is known to be efficacious in fever, liver diseases, bronchitis, infantile convulsions and inflammations (The Wealth of India, 1950). Systematic investigations on the seeds of plant *Cleome viscosa* has resulted in the isolation of coumarino-lignoids, cleomiscosin A, B and C. It is a novel class of natural products in which a lignan (C₆–C₃) unit is linked with a coumarin moiety through a dioxane bridge having hepatoprotective activity (Chattopadhyay et al., 1999). The effect of coumarino-lignoid, cleomiscosin A, B and C isolated from the plant *Cleome viscosa* on inflammatory mediators was earlier studied by our group in female swiss albino mice. The result of this study concluded that the oral administration of coumarino-lignoids inhibited the pro-inflammatory mediators and enhanced the production of anti-inflammatory mediator in a dose dependent manner (Bawankule et al., 2008). In our previous publication (Sharma et al., 2010), we reported the synthesis of six novel cleomiscosin A analogs and their corresponding methyl ether derivatives. The result of *in vitro* target based anti-inflammatory study using primary macrophages cell culture bioassay system showed that only the halogenated derivatives, **1a** (5-Bromo-9' acetate) cleomiscosin A, **3a** (5-Chloro) cleomiscosin A methyl ether and **4a** (5-Bromo)cleomiscosin A methyl ether exhibited potent anti-inflammatory activity when compared with diclofenac sodium taken as a control (Sharma et al., 2010). This prompted us to synthesize several novel polyhalogenated derivatives of cleomiscosin A methyl ether (Cliv-M) (Ray et al., 1985) using a modified method of Surya Prakash et al. (2004) in order to study the anti-inflammatory effects on various pro-inflammatory targets.

In present communication, anti-inflammatory drug-like potential of Cliv-M derivatives (**6a–9a**) have been discussed on the basis of their *in silico* and *in vitro* activity studies.

2. Materials and methods

2.1. Chemistry and instrument

All reagents were commercial and used without further purification. Column chromatography was carried on silica gel (60–120 and 100–200 mesh). TLC has monitored all reactions; silica gel plates with fluorescence F₂₅₄ were used. Melting points were determined in open capillaries on a JSGW melting point apparatus and are uncorrected. All the chemicals, reagents (BF₃-Et₂O, N-halosuccinimides, Dimethyl carbonate) and solvents were obtained from LobaChemie, Qualigens, MERCK and used as such. The purity of the compounds were checked on TLC (Silica gel 60 F₂₅₄). All the products were characterized by ¹H NMR (Bruker AVANCE 300 MHz), and ¹³C NMR (Bruker AVANCE 75 MHz, FT NMR) using CDCl₃ and TMS as internal standard. Chemical shifts are reported in parts per million. Splitting patterns are described as singlet (s), broad singlet (brs), doublet (d), broad doublet (brd), double doublet (dd), triplet (t), quartet (q), and multiplet (m). IR spectra (KBr pellets) 600–4000 cm⁻¹, were recorded on Perkin Elmer FTIR, BX spectrophotometer and Mass Spectra (Electrospray ionization in positive mode, ESI+) were recorded on an API 3000 (Applied Biosystem) mass spectrometer. All the synthesized compounds gave satisfactory elemental analysis (carbon, hydrogen and nitrogen).

2.2. General procedure for the synthesis of (3,5,2' trichloro)cleomiscosin A methyl ether (**6a**)/(5,6' dichloro)cleomiscosin A methyl ether (**6b**)/(3,5,5',6' tetrabromo)cleomiscosin A methyl ether (**7a**)/(3,5,5' triiodo)cleomiscosin A methyl ether (**8a**)/(5,6' diiodo)cleomiscosin A methyl ether (**8b**)

BF₃-Et₂O (4.0 ml, 32.4 mmol) was added to a mixture of the cleomiscosin A methyl ether (50 mg, 0.10 mmol) and N-halosuccinimide (50 mg, 0.30 mmol) in a 50 mL round bottom flask. The reaction R.B. was closed and the mixture was stirred at room temperature for a specified period of time (3–4 h). After completion of the reaction, the reaction mixture then completely transferred to a separating funnel using water (20 mL) and dichloromethane (2 × 20 mL) and thoroughly shaken to extract the product into the organic layer. The organic layer was then washed with saturated solution of sodium bisulfate (15 mL) to remove any free halogen present followed by saturated bicarbonate solution (20 mL) and brine (20 mL). It was then washed with water (2 × 20 mL) and dried over anhydrous sodium sulfate. The solvent was removed under reduced pressure and the product was purified by column chromatography (silica gel, 60–120 mesh, petroleum ether/ethyl acetate, 70:30, 60:40, 50:30) to afford the desired polyhalogenated derivatives. The crude product was then recrystallized from ethyl acetate/hexane.

2.2.1. (3,5,2' Trichloro)cleomiscosin A methyl ether (**6a**)

Light yellow solid (30.0 mg, 47.7%), m.p. 83–85 °C, IR (KBr): ν_{\max} = 3443, 1739, 1604, 1569, 1473, 1448, 1390, 1260, 1168, 1070 cm⁻¹. Mass (ESI +) [M + H]⁺/[M + 2 + H]⁺: m/z = 503/505. ¹H NMR (CDCl₃, 300 MHz, 25 °C): δ = 8.16 (s, 1H, 4H), 6.92 (d, J = 12.9 Hz, 1H, 5'H), 6.88 (d, J = 12.9 Hz, 1H, 6'H), 5.50 (d, J = 8.1 Hz, 1H, 7'H), 4.35 (m, 1H, 8'H), 3.97 (m, 2H, 9'H), 3.91 (s, 3H, -OCH₃), 3.99 (2s, 2 × 3H, 2 × -OCH₃) ppm. ¹³C NMR (CDCl₃, 75 MHz, 25 °C): δ = 156.5 (C-2), 120.8 (C-3), 137.7 (C-4), 116.1 (C-5), 142.8 (C-6), 141.8 (C-7), 130.8 (C-8), 139.0 (C-9), 110.8 (C-10), 125.2 (C-1'), 123.9 (C-2'), 150.5 (C-3'), 148.7 (C-4'), 112.8 (C-5'), 111.1 (C-6'), 74.2 (C-7'), 78.3 (C-8'), 61.5 (C-9'), 61.8, 56.6, 56.7 (3 × -OCH₃) ppm.

2.2.2. (5,6' Dichloro)cleomiscosin A methyl ether (**6b**)

Light yellow solid (22.0 mg, 37.6%), m.p. 132–133 °C, IR (KBr): ν_{\max} = 3387, 2919, 1731, 1606, 1571, 1513, 1466, 1436, 1310, 1298, 1263, 1212, 1065, 823, 636 cm⁻¹. Mass (ESI +) [M + H]⁺/[M + 2 + H]⁺: m/z = 469/471, [M + Na]⁺: m/z = 491/493, [M + K]⁺: m/z = 507/509. ¹H NMR (CDCl₃, 300 MHz, 25 °C): δ = 6.40 (d, J = 9.9 Hz, 1H, 3H), 8.00 (d, J = 9.9 Hz, 1H, 4H), 6.92 (s, 1H, 2'H), 6.89 (s, 1H, 5'H), 5.50 (d, J = 8.1 Hz, 1H, 7'H), 4.34 (m, 1H, 8'H), 3.88–3.91 (m, 2H, 9'H), 3.91 (s, 3H, -OCH₃), 3.82 (2s, 2 × 3H, 2 × -OCH₃) ppm. ¹³C NMR (CDCl₃, 75 MHz, 25 °C): δ = 160.2 (C-2), 115.1 (C-3), 140.8 (C-4), 117.4 (C-5), 142.6 (C-6), 140.9 (C-7), 131.2 (C-8), 141.8 (C-9), 111.1 (C-10), 125.6 (C-1'), 113.2 (C-2'), 150.8 (C-3'), 149.0 (C-4'), 111.5 (C-5'), 124.6 (C-6'), 74.5 (C-7'), 78.6 (C-8'), 61.5 (C-9'), 61.7, 56.7, 56.5 (3 × -OCH₃) ppm.

2.2.3. (3,5,5',6' Tetrabromo)cleomiscosin A methyl ether (**7a**)

White solid (40.0 mg, 44.8%), m.p. 146–148 °C, IR (KBr): ν_{\max} = 3442, 2934, 1735, 1600, 1563, 1472, 1436, 1384, 1070, 915, 898, 752, 654 cm⁻¹. Mass (ESI +) [M + H]⁺: m/z = 713. ¹H NMR (CDCl₃, 300 MHz, 25 °C): δ = 8.40 (s, 1H, 4H), 6.96 (s, 1H, 2'H), 5.60 (d, J = 7.8 Hz, 1H, 7'H), 4.36 (m, 1H, 8'H), 3.88–3.99 (m, 2H, 9'H), 3.89 (s, 3H, -OCH₃), 3.88 (2s, 2 × 3H, 2 × -OCH₃) ppm. ¹³C NMR (CDCl₃, 75 MHz, 25 °C): δ = 156.3 (C-2), 110.4 (C-3), 143.9 (C-4), 106.5 (C-5), 147.2 (C-6), 141.1 (C-7), 131.2 (C-8), 139.9 (C-9), 122.9 (C-10), 131.4 (C-1'), 111.9 (C-2'), 149.0 (C-3'), 153.2 (C-4'), 112.7 (C-5'), 117.1 (C-6'), 77.4 (C-7'), 78.5 (C-8'), 61.0 (C-9'), 61.3, 60.6, 56.4 (3 × -OCH₃) ppm.

2.2.4. (3,5,5'-Triiodo)cleomiscosin A methyl ether (**8a**)

Pale yellow solid (36.6 mg, 37.6%), m.p. 144–145 °C, IR (KBr): ν_{\max} = 3424, 2918, 1721, 1596, 1509, 1434, 1254, 1166, 1077, 1025, 884, 748, 670, 628 cm^{-1} . Mass (ESI +) $[M + H]^+$: m/z = 779, $[M + Na]^+$: m/z = 801, $[M + K]^+$: m/z = 817. ^1H NMR (CDCl_3 , 300 MHz, 25 °C): δ = 8.54 (s, 1H, 4H), 7.31 (s, 1H, 2'H), 6.82 (s, 1H, 6'H), 5.30 (d, J = 8.1 Hz, 1H, 7'H), 4.34 (brs, 1H, 8'H), 3.86–3.99 (m, 2H, 9'H), 3.85 (s, 3H, $-\text{OCH}_3$), 3.90 (2s, $2 \times 3\text{H}$, $2 \times -\text{OCH}_3$) ppm. ^{13}C NMR (CDCl_3 , 75 MHz, 25 °C): δ = 157.0 (C-2), 82.8 (C-3), 156.5 (C-4), 84.5 (C-5), 146.1 (C-6), 140.5 (C-7), 132.1 (C-8), 140.7 (C-9), 115.8 (C-10), 129.4 (C-1'), 111.2 (C-2'), 150.1 (C-3'), 150.6 (C-4'), 87.4 (C-5'), 122.0 (C-6'), 81.0 (C-7'), 79.3 (C-8'), 61.6 (C-9'), 61.6, 56.6, 56.7 ($3 \times -\text{OCH}_3$) ppm.

2.2.5. (5,6'-Diiodo)cleomiscosin A methyl ether (**8b**)

Dark yellow solid (35.0 mg, 42.9%), m.p. 152–153 °C, IR (KBr): ν_{\max} = 3429, 2919, 1724, 1596, 1505, 1513, 1432, 1374, 1256, 1064, 982, 839, 778, 750, 599 cm^{-1} . Mass (ESI +) $[M + H]^+$: m/z = 653, $[M + Li]^+$: m/z = 659, $[M + Na]^+$: m/z = 675, $[M + K]^+$: m/z = 691. ^1H NMR (CDCl_3 , 300 MHz, 25 °C): δ = 6.20 (d, J = 9.9 Hz, 1H 3H), 7.80 (d, J = 9.9 Hz, 1H, 4H), 6.79 (s, 1H, 2'H), 7.23 (s, 1H, 5'H), 5.30 (d, J = 8.1 Hz, 1H, 7'H), 4.30 (m, 1H, 8'H), 4.00 (m, 2H, 9'H), 3.83 (s, 3H, $-\text{OCH}_3$), 3.79 (2s, $2 \times 3\text{H}$, $2 \times -\text{OCH}_3$) ppm. ^{13}C NMR (CDCl_3 , 75 MHz, 25 °C): δ = 160.0 (C-2), 115.6 (C-3), 148.0 (C-4), 84.6 (C-5), 146.2 (C-6), 140.6 (C-7), 132.6 (C-8), 141.2 (C-9), 114.9 (C-10), 129.9 (C-1'), 111.7 (C-2'), 150.5 (C-3'), 150.9 (C-4'), 122.5 (C-5'), 87.9 (C-6'), 80.9 (C-7'), 79.3 (C-8'), 61.7 (C-9'), 61.5, 56.7, 56.6 ($3 \times -\text{OCH}_3$) ppm.

2.3. General procedure for the synthesis of 9' methyl ester of cleomiscosin A methyl ether (**9a**)

A mixture of cleomiscosin A methyl ether (100 mg, 0.30 mmol), potassium carbonate (50 mg, 41.4 mmol), dimethyl carbonate (5 mL, 0.06 mol) and N,N-dimethyl formamide (5 mL) in a 100 mL round bottom flask was refluxed at 100 °C for 24 h. After completion of reaction, the reaction mixture was then cooled to 0 °C. Water (50 mL), was added which resulted in the formation of a precipitate. The mixture was stirred at -5 °C for 1 h, then the solid was collected by filtration washed with water (50 mL) and dried under high vacuum to give a methyl ester derivative of cleomiscosin A methyl ether.

2.3.1. 9' Methyl ester of cleomiscosin A methyl ether (**9a**)

White solid (42.0 mg, 36.7%), m.p. 158–160 °C, IR (KBr): ν_{\max} = 3422, 2959, 1751, 1718, 1577, 1508, 1458, 1304, 1269, 1141, 1025, 942, 791, 766 cm^{-1} . Mass (ESI +) $[M + H]^+$: m/z = 459, $[M + Na]^+$: m/z = 481. ^1H NMR (CDCl_3 , 300 MHz, 25 °C): δ = 6.30 (d, J = 9.3 Hz, 1H, 3H), 8.60 (d, J = 9.6 Hz, 1H, 4H), 6.53 (s, 1H, 5H), 7.00 (dd, J = 8.1 Hz, 1H, 2'H), 6.90 (dd, J = 8.7, 1H, 5'H), 6.87 (dd, J = 8.7, 1H, 6'H), 5.00 (d, J = 7.8 Hz, 1H, 7'H), 4.05–4.10 (dd, J = 3.6, 12.0 Hz, 1H, 8'H), 4.35–4.49 (m, J = 2.1, 12.0 Hz, 2H, 9'H), 3.88 (s, 9H, $-\text{OCH}_3$), 3.79 (s, 3H, $-\text{OCH}_3$) ppm. ^{13}C NMR (CDCl_3 , 75 MHz, 25 °C): δ = 160.6 (C-2), 111.4 (C-3), 143.6 (C-4), 114.3 (C-5), 145.8 (C-6), 137.1 (C-7), 131.8 (C-8), 138.7 (C-9), 111.8 (C-10), 126.9 (C-1'), 110.3 (C-2'), 150.0 (C-3'), 149.4 (C-4'), 100.4 (C-5'), 120.3 (C-6'), 75.4 (C-7'), 76.2 (C-8'), 65.7 (C-9'), 155.1 (C=O), 55.7, 56.3, 54.9, 53.7 ($4 \times -\text{OCH}_3$) ppm.

2.4. Structure cleaning and molecular docking

Drawing and geometry cleaning of the series of compounds was performed through ChemBioDraw-Ultra-v12.0 (<http://www.cambridge-soft.com/>). The 2D structures has transformed into 3D structures using converter module of ChemBioDraw. The 3D structures then subjected to energy minimization, which has performed in

two steps. In the first step energy minimized using molecular mechanics-2 (MM2) until the root mean square (RMS) gradient value became smaller than 0.100 kcal/mol Å then in second step minimized MM2 (dynamics) compounds were subjected to re-optimization through MOPAC (Molecular Orbital Package) method until the RMS gradient attained a value smaller than 0.0001 kcal/mol Å.

The 3D chemical structures of known drugs have retrieved from the PubChem compound database at NCBI (<http://www.pubchem.ncbi.nlm.nih.gov>). Crystallographic 3D structures of target proteins have retrieved from the Brookhaven Protein Databank (<http://www.pdb.org>). The valency and hydrogen bonding of each ligand as well as each target protein were subsequently checked using the Workspace module of the Scigress Explorer software. Hydrogen atoms were added to the protein targets to achieve the correct ionization and tautomeric states of amino acid residues such as His, Asp, Ser, and Glu. Molecular docking of the standard compounds/drugs and studied derivatives against selected targets was achieved using the FastDock Manager and FastDock Compute engines of Scigress Explorer v.7.7.0.47 software (previously, CAChe) (Fujitsu Ltd., Poland, <http://www.fqs.pl/>). To perform the automated docking of ligands into the active sites, we used a genetic algorithm with a fast and simplified potential of mean force (PMF) scoring scheme (Muegge, 2000; Martin, 1999). PMF uses atom types that are similar to the empirical force fields used in mechanics and dynamics. A minimization has performed by the FastDock engine, which uses a Lamarkian genetic algorithm (LGA) so that individuals adapt to the surrounding environment. The best fits sustained by analyzing the PMF scores of all chromosomes and assigning more reproductive opportunities to those with lower scores. This process was repeated for 3000 generations with 500 individuals and 100,000 energy evaluations. Other parameters were left as their default values. Structure-based screening involves docking of candidate ligands into protein targets and then applying a PMF scoring function to estimate the likelihood that the ligand will bind to the protein with high affinity or not (Muegge, 2000; Martin, 1999; Yadav et al., 2010, 2011; Meena et al., 2011).

2.5. Parameters for QSAR model development

Initially, 34 anti-inflammatory drugs/compounds (see Supplementary Table 1) with reported activities have used in training data set while developing the QSAR model. The anti-inflammatory activity was in inhibitory concentration (IC_{50} in nM) form. Total 52 chemical descriptors (physico-chemical properties) (see Supplementary Table 2) were calculated for each compound. The Scigress Explorer software (Fujitsu, Poland) calculated descriptors like electronic, steric and thermodynamic. Compounds selection has based on structural similarity, to ensure diverse training data set rather than same family. On the basis of small molecules structural similarity, compounds selection was performed so that to ensure diverse training data set. While selecting the best subset of chemical descriptors, highly correlated descriptors were excluded by using correlation matrix (see Supplementary file 3) approach or co-variance analysis.

Similarly, when selecting the best subset of chemical descriptors, highly correlated descriptors developed based on forward stepwise multiple linear regression method. The resulting QSAR model exhibited a high regression coefficient. The model was successfully validated using random test set compounds, and evaluated for the robustness of its predictions via the cross-validation coefficient. Validation of QSAR models used "Leave-one-out (LOO)" method (Yadav et al., 2010, 2011; Meena et al., 2011). The best model selection was based on various statistical parameters such as correlation coefficient (r), square of correlation

coefficient (r^2), quality of the each model was estimated from the cross-validated squared correlation coefficient (r_{CV}^2), which confirm the robustness and applicability of QSAR equation.

2.6. Screening through pharmacokinetic properties

The ideal oral drug is one that rapidly and completely absorbed from the gastrointestinal tract, distributed specifically to its site of action in the body, metabolized in a way that does not instantly remove its activity, and eliminated in a suitable manner without causing any harm. It has reported that around half of all drugs in development fail to make it to the market because of poor pharmacokinetics (PK) (Hodgson, 2001). The PK properties depend on the chemical properties of the compound. PK properties such as absorption, distribution, metabolism, excretion, and toxicity (ADMET) are important determinants of the success of the compound for human therapeutic use (Hodgson, 2001; Sean et al., 2006; Norinder and Bergström, 2006). Some important chemical descriptors correlate well with PK properties, such as the polar surface area (PSA, a primary determinant of fractional absorption) and low molecular weight (MW, for oral absorption) (Reichel and Begley, 1998). The distribution of the compound in the human body depends on factors such as the blood–brain barrier ($\log BB$), permeability (such as the apparent Caco-2 permeability, apparent MDCK permeability, $\log Kp$ for skin permeability), the volume of distribution and plasma protein binding ($\log K_{hsa}$ for serum protein binding) (Reichel and Begley, 1998). These parameters were calculated by QikProp v.3.2 software (Schrodinger, USA, 2009) and checked for compliance with their standard ranges. The octanol–water partition coefficient ($\log P$) implicated in BBB penetration and permeability prediction, as has PSA. It was reported that the process of excreting the compound from the human body depends on the MW and $\log P$. Likewise, rapid renal clearance is associated with small and hydrophilic compounds. On the other hand, the metabolism of most drugs, which takes place in the liver, is associated with large and hydrophobic compounds (Lombardo et al., 2003). Higher compound lipophilicity leads to increased metabolism and poor absorption, along with an increased probability of binding to unwanted hydrophobic macromolecules, thereby increasing the potential for toxicity. In spite of some observed exceptions to Lipinski's rule, the property values of the vast majority (90%) of orally active compounds are within their cut-off limits (Lipinski et al., 2001). Molecules that violate more than one of these rules may not be sufficiently bioavailable. When studying PK properties, screening based on Lipinski's rule of five (which has used to assess drug likeness) has applied to the Cliv-M derivatives. In addition, the bioavailability of each derivative was assessed through its topological polar surface area (TPSA) using ChemAxon's MarvinView 5.2.6: PSA plugin software (<http://www.chemaxon.com>) (Ertl et al., 2000; Veber et al., 2002; Clark, 1999). This descriptor shown to correlate well with passive molecular transport through membranes, thus allowing the prediction of drug transports properties, and it has linked to drug bioavailability (the percentage of the dose of the drug that reaches the blood circulation). In addition, the number of rotatable bonds is a simple topological parameter used by researchers as part of an extended Lipinski's rule of five as a measure of molecular flexibility. This is a very good chemical descriptor for oral bioavailability (Ertl et al., 2000; Veber et al., 2002; Clark, 1999). A rotatable bond is defined as any single non-ring bond bound to a non-terminal heavy (i.e., non-hydrogen) atom. Amide C–N bonds are not considered in this context because of their high rotational energy barrier. Moreover, some researchers have also included the sum of H-bond donors and H-bond acceptors as a secondary determinant of fractional absorption. The primary determinant of fractional absorption is PSA (Clark, 1999). According to the extended

Lipinski's rule of five, the sum of H-bond donors and acceptors should be ≤ 12 or the PSA should be $\leq 140 \text{ \AA}^2$, and the number of rotatable bonds should be ≤ 10 (Veber et al., 2002).

2.7. In vitro anti-inflammatory study

Inflammation is a multi-step process that is mediated by activated inflammatory cells, including macrophages/monocytes (Minagar et al., 2002). In the presence of stimuli such as lipopolysaccharide (LPS), activated macrophages induce the overproduction of pro-inflammatory cytokines such as TNF- α , IL-1 β and IL-6 (Jung et al., 2007). In this study, we used macrophage cells stimulated with LPS for target based *in vitro* anti-inflammatory evaluation of compounds **6a–9a**. The compounds (**6a–9a**) were dissolved in DMSO at a concentration of 1 and 10 $\mu\text{g/mL}$. Primary macrophage cells were collected from the peritoneal cavities of mice (8-week-old female Swiss albino mice) after an intra-peritoneal (i.p.) injection of 1 mL of 1% peptone (BD USA) 3 days before harvesting. Mice were euthanized by cervical dislocation under ether anesthesia and peritoneal macrophages were obtained by intra-peritoneal (i.p.) injection of Phosphate Buffer Saline (PBS), pH-7.4. The peritoneal macrophages at the concentration of 2.5×10^5 live cells/mL were used for the experimentation.

2.7.1. Quantification of pro-inflammatory mediators using Enzyme-Linked Immunosorbent Assay (ELISA)

The cells were suspended in RPMI 1640 medium (Sigma Chemicals Co., USA) containing 10% heat-inactivated fetal calf serum (Gibco, USA), 100 U/mL of penicillin and 100 mg/mL of streptomycin and incubated in a culture plate (Nunc, Germany) at 37 °C in 5% CO₂ in an incubator. Non-adherent cells removed after 2 h and the adherent cells resuspended in RPMI 1640 medium. Cells were pre-treated with (1 and 10 $\mu\text{g/mL}$) of test compounds, 30 min before the stimulation with lipopolysaccharide (LPS, 0.5 $\mu\text{g/mL}$). After incubation with LPS for 24 h, supernatants collected and immediately frozen at –80 °C. Harvested supernatants tested for quantification of pro-inflammatory mediators (IL-1 β , IL-6 and TNF- α) by ELISA using commercial kits for mouse IL-1 β , IL-6 and TNF- α (BD Biosciences, USA). All the synthesized derivatives dissolved in dimethyl sulphoxide (DMSO) and cells treated with 10 μL of DMSO were considered as a vehicle control. *In vitro* anti-inflammatory activity of the compounds was compared with vehicle control (Sharma et al., 2010).

2.7.2. Cell viability assay

Cell viability assay carried out in similar conditions where the experiments for anti-inflammatory activity were done. Cell viability was determined by using the 3-(4,5-dimethylthiazol-2-yl)-2,5-diphenyltetrazolium (MTT) assay. Murine Peritoneal Macrophage Cells (0.25×10^5 cells/mL) were suspended in RPMI 1640 medium (Sigma Chemicals Co., USA) containing 10% heat-inactivated fetal bovine serum (Gibco, USA), 100 U/mL of penicillin and 100 mg/mL of streptomycin and incubated in a culture 96 well plate (Nunc, Germany) at 37 °C in 5% CO₂ in an incubator. 20 μL aliquots of **6a–9a** solutions (10,100 and 1000 $\mu\text{g/mL}$) were added to each well using DMSO as solvent. Cells incubated in culture medium alone served as a control for cell viability (untreated wells). After incubation, cells with treatment compounds for 24 h, 20 μL aliquots of MTT solution (5 mg/mL in PBS) added to each well. Then, the 200 μL of supernatant culture medium were carefully aspirated and 200 μL aliquots of dimethylsulfoxide (DMSO) added to each well to dissolve the formazan crystals, following by incubation for 10 minutes to dissolve air bubbles. The culture plate was placed on a micro-plate reader (Spectramax, Molecular Devices, USA) and the absorbance was measured at 550 nm. The purple color produced is directly proportional to the number of viable cell. All

assays performed in six replicates for each concentration. Cell viability rate was calculated as the percentage of MTT absorption as follows: % survival = (mean experimental absorbance/mean control absorbance × 100) (Brown et al., 2008).

3. Results and discussion

3.1. Chemistry of novel cleomiscosin A methyl ether (Cliv-M) derivatives

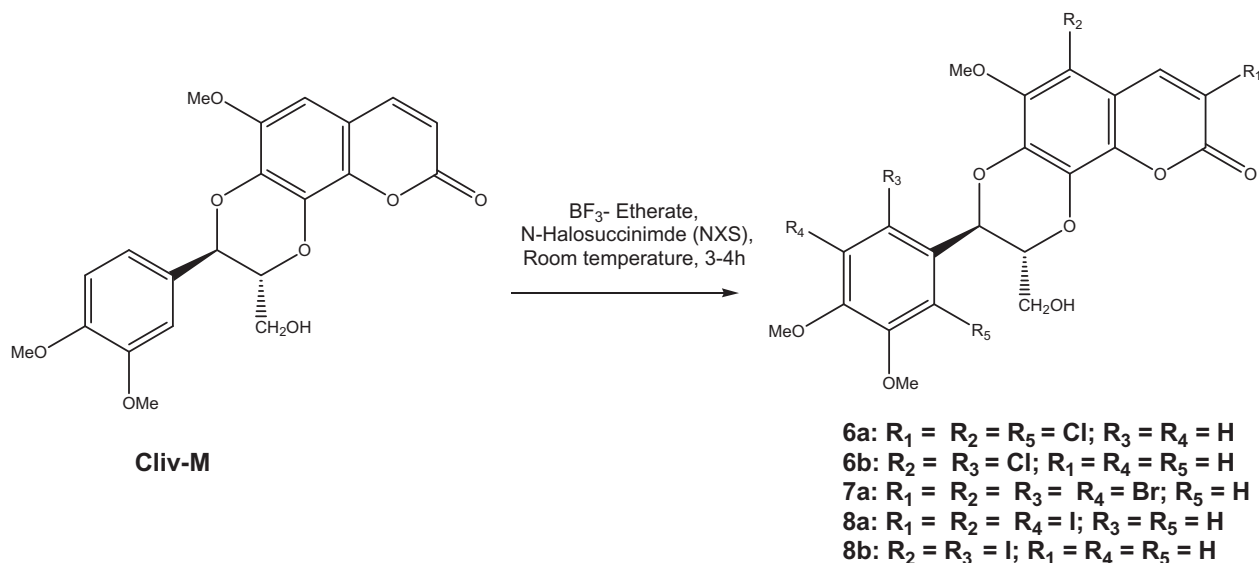
The syntheses of five new cleomiscosin A methyl ether derivatives (**6a**, **6b**, **7a**, **8a** and **8b**) were accomplished with BF₃-Et₂O and N-halosuccinimides through the synthetic route reported in Scheme 1. The reaction of Cliv-M with N-halosuccinimides, NXS (X = Cl, Br, I) in the presence of BF₃-Et₂O at room temperature produced trichloro, tetrabromo, triiodo and diiodo derivatives of Cliv-M. We have studied the halogenation of Cliv-M using a combination of NXS and BF₃-Et₂O at room temperature. This halogenation method developed as a modification of an earlier method reported by Surya Prakash et al. (Surya Prakash et al., 2004; Olah et al., 1989, 2001; Olah, 1993).

The reaction of Cliv-M with N-chlorosuccinimide and BF₃-Et₂O at room temperature converted it into two chloro derivatives, one was a trichlorinated derivative, **6a** and other one was the dichlorinated derivative, **6b** of Cliv-M (Scheme 1). The trichlorinated derivative, **6a** (C₂₁H₁₇O₈Cl₃, m.p. 83–85 °C), [M + H]⁺ and [M + 2 + H]⁺ at *m/z* 503 and 505, in its ¹H NMR spectrum showed the presence of only three aromatic protons. The absence of coumarin C-3 proton and therefore the absence of diagnostic coupling constant of *J* = 10 Hz between C-3H and C-4H indicated the attachment of a Cl atom to C-3 position. Also from the ¹H NMR, the attachment of second Cl atom was confirmed at C-5 position. This finding has established because of the downfield shift of C-4H from the original value of δ 7.62–8.16 ppm and it appeared as a singlet. The third Cl atom was introduced into the phenyl propane unit at C-2'H position which was evident from the presence of three more signals for quaternary carbons in its ¹³C NMR spectrum and absence of three –CH signals for three aromatic protons. The structure of second minor dichloro derivative, C₂₁H₁₈O₈Cl₂, m.p.

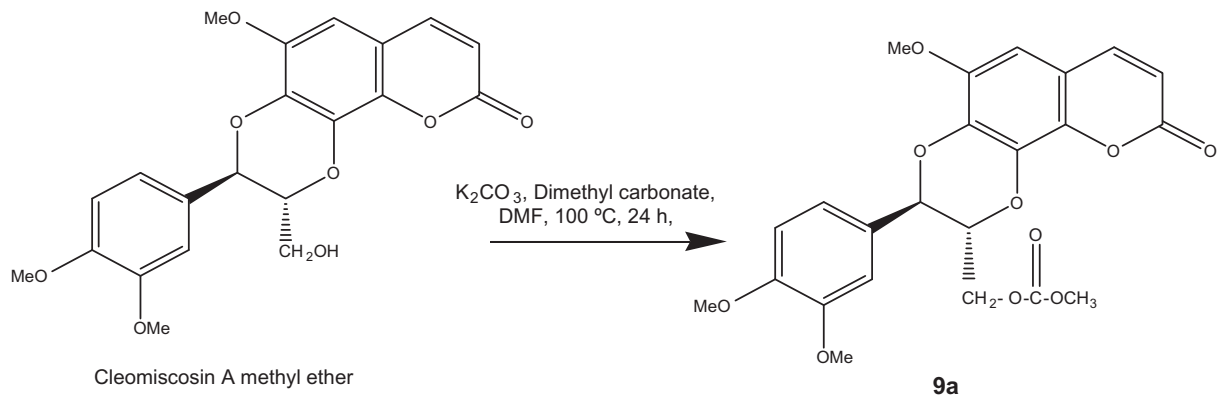
132–133 °C, was confirmed as **6b**, as it showed the downfield shift of the C-4H which appeared at δ 8.00 (d, *J* = 9.9 Hz) and also showed the absence of C-5H in its ¹H NMR spectrum which confirmed the attachment of one Cl atom at C-5 position. The other Cl atom was put at C-6' position as C-5'H and C-2'H appeared as singlets at δ 6.89 and 6.92 ppm respectively.

The tetrabromo derivative **7a** of Cliv-M was obtained when Cliv-M was stirred with N-bromosuccinimide and BF₃-Et₂O at room temperature for 2 h. Only one product has formed, which was found to contain four Br atoms attached to coumarin and phenyl propane unit (C₆–C₃ unit). The ESI-MS (positive mode) of **7a**, C₂₁H₁₆O₈Br₄, m.p. 146–148 °C, showed [M + H]⁺ at *m/z* 713. Moreover, the MS/MS spectrum showed two distinctive peaks, one at *m/z* 697.5 that has obtained by the loss of a H₂O molecule from the parent M⁺ 713. Second major peak obtained from the retro Diels-Alder cleavage of the parent molecule that gave two peaks at *m/z* 362 and 310.8. The ¹H NMR spectrum of **7a** displayed two singlets for two aromatic protons at δ 8.40 and 6.96 for C-4H and C-2'H, respectively. In its ¹³C NMR spectrum, four quaternary carbon signals appeared at δ 110.4, 106.5, 112.7 and 117.1 for C-3, C-5, C-5' and C-6' respectively. Thus, based on NMR and mass spectral data, structure **7a** was assigned to the tetrabromo derivative of Cliv-M.

In order to explore the reactivity of Cliv-M towards iodination reaction, Cliv-M was treated with N-iodosuccinimide and BF₃-Et₂O at room temperature to give two iodo derivatives **8a** and **8b**. Compound **8a**, C₂₁H₁₇O₈I₃, [M + H]⁺: *m/z* 779, [M + Na]⁺: *m/z* 801 and [M + K]⁺: *m/z* 817, m.p. 144–145 °C, was a triiodo derivative. Its ¹H NMR spectrum showed signals for three aromatic protons at δ 8.54, 7.31 and 6.82 ppm for C-4H, C-2' H and C-6' H, and the absence of coupling between the C-3 and C-4 protons. Furthermore, the downfield chemical shift of C-4 proton was ascertained due to the presence of another iodo group at C-5H position. The position of third iodo group at C-5'H position was confirmed by HSQC and HMBC correlations. Compound **8b**, (C₂₁H₁₈O₈I₂, m.p. 152–153 °C), was a diiodo derivative. Its ESI-MS (positive mode) spectrum showed [M + H]⁺ at *m/z* 653, [M + Li]⁺ at *m/z* 659, [M + Na]⁺ at *m/z* 675 and [M + K]⁺ at *m/z* 691. The ¹H NMR of compound **8b** showed the presence of two singlets at δ 6.79 and 7.23 indicating that C-2'H and C-5'H were intact. The two iodo



Scheme 1. Reagents and conditions: cleomiscosin A methyl ether (0.10 mmol), N-halosuccinimide (NXS, X = Cl, Br, I) (0.30 mmol), BF₃-Et₂O (4.0 ml, 32.4 mmol), 3–4 h, room temperature.



Scheme 2. Reagents and conditions: cleomiscosin A methyl ether (0.30 mmol), potassium carbonate (41.4 mmol), dimethyl carbonate (5 ml, 0.06 mol) and N,N-dimethyl formamide (5 ml), reflux, 100 °C, 24 h.

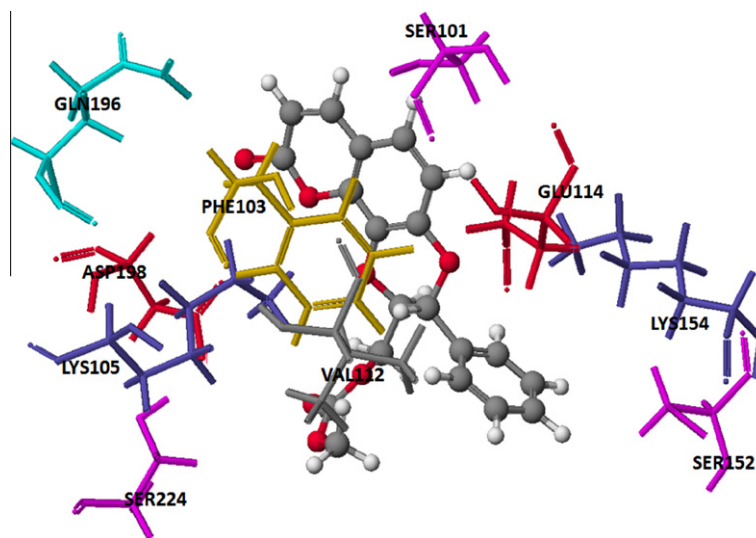


Fig. 1. Compound 9a docked on anti-inflammatory target IL6 (PDB: 1N26) with high binding affinity docking score -92.450 kcal/mol.

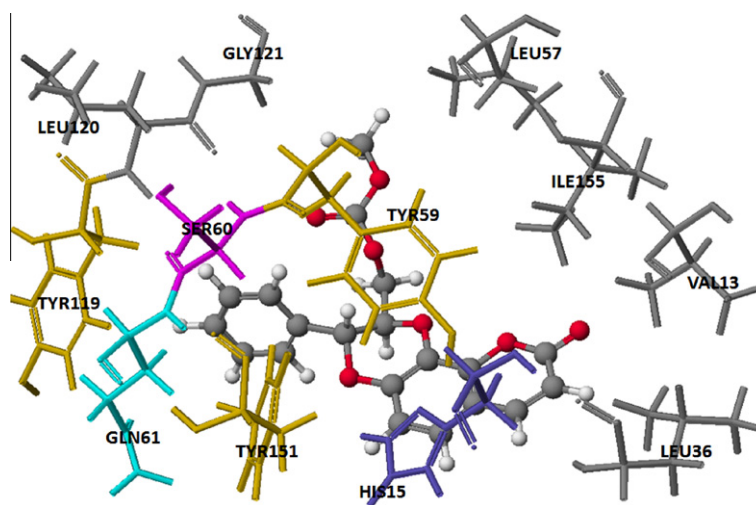


Fig. 2. Compound 9a docked on anti-inflammatory target TNF- α (PDB: 2A25) with high binding affinity docking score -94.992 kcal/mol.

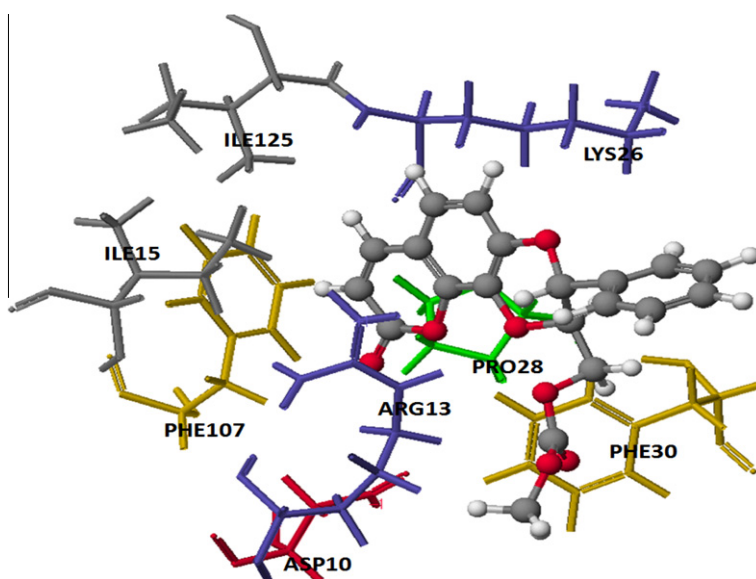


Fig. 3. Compound **9a** docked on anti-inflammatory target IL1- β (PDB: 3O40) with high binding affinity docking score -67.462 kcal/mol.

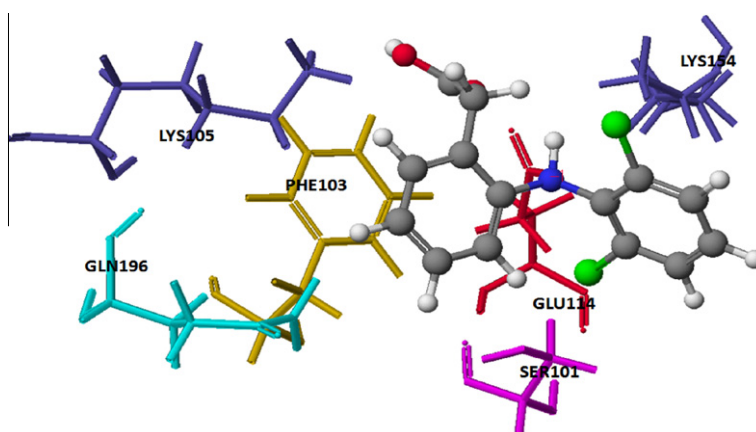


Fig. 4. Diclofenac sodium docked on anti-inflammatory target IL6 (PDB: 1N26) with high binding affinity docking score -64.141 kcal/mol.

groups were positioned at C-6'H and C-5H. Finally, the structure of **8b** was confirmed by its ^{13}C NMR and DEPT 135° experiments.

We have also studied the reactivity of primary alcoholic group of Cliv-M (Scheme 2). When it was refluxed with potassium carbonate, dimethyl carbonate and DMF at 100°C for 24 h, an ester derivative of cleomiscosin A methyl ether was obtained. When the same reaction has performed with cleomiscosin A, no product was formed. The structure of compound **9a** ($\text{C}_{23}\text{H}_{22}\text{O}_{10}$, m.p. $158\text{--}160^\circ\text{C}$) was confirmed by spectral analysis. The IR of **9a** showed a carbonyl band at 1751 cm^{-1} . The ^1H NMR spectrum of **9a** showed a singlet at δ 3.72 for $-\text{OMe}$ group of ester and ^{13}C NMR showed a carbonyl group at δ 155.1.

3.2. Chemical structure–activity relationship

The QSAR results indicated that studied Cliv-M derivatives (**6a–9a**) showed activity levels similar to or higher than that of standard drugs. Thus, we designed and virtually optimized a number of Cliv-M derivatives (**6a–9a**) based on the conformational restricted functional moiety as a basic unit along with different halogen atoms and groups at the different carbon position. We

Table 1

Docking scores (kcal mol^{-1}) of Cliv-M (**6a–9a**) derivatives with respect to the anti-inflammatory targets IL-6, TNF- α and IL-1 β .

| Drugs/compounds | Docking energy (kcal/mol) with anti-inflammatory receptors | | |
|-------------------|---|---------------|--------------|
| | IL-6 | TNF- α | IL-1 β |
| Cleomiscosin A | -90.302 | -35.912 | -71.958 |
| Cliv-M | -96.164 | -94.913 | -85.15 |
| 6a | -81.933 | -69.235 | -65.985 |
| 6b | -83.302 | -45.258 | -80.327 |
| 7a | -93.787 | -45.873 | -77.38 |
| 8a | -90.939 | -90.881 | -84.447 |
| 8b | -99.394 | -96.377 | -65.367 |
| 9a | -92.45 | -94.992 | -67.462 |
| Diclofenac sodium | -64.141 | -76.282 | -62.091 |
| Ibuprofen | -56.248 | -63.135 | -49.712 |
| Aristolochic | -73.067 | -88.284 | -73.588 |
| Indometacin | -74.086 | -30.964 | -54.819 |

report the anti-inflammatory activity of these newly designed derivatives with the basic pharmacophore, which were found to be comparable to potent standard compounds. Figs. 1–4 show

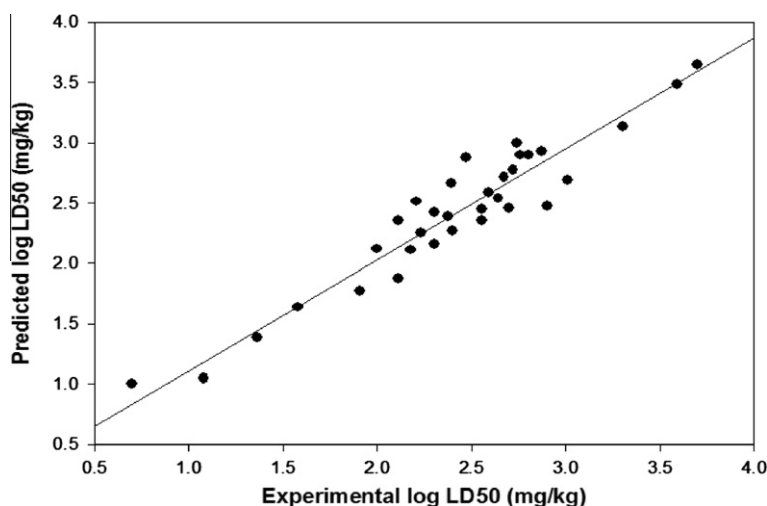


Fig. 5. Multiple linear regression curve showing linear relationship between values of experimental and predicted logLD₅₀ calculated by derived QSAR model.

Table 2

Predicted anti-inflammatory activity (LD₅₀ mg/kg) of Cliv-M (6a–9a) derivatives and its virtual screening.

| Drug/compounds | Predicted logLD ₅₀ (mg/kg) | Predicted LD ₅₀ (mg/kg) |
|-------------------|---------------------------------------|------------------------------------|
| Cleomiscosin A | 3.789 | 6151.77 |
| Cliv-M | 2.436 | 272.90 |
| 6a | 2.467 | 293.09 |
| 6b | 2.803 | 635.33 |
| 7a | 2.543 | 349.14 |
| 8a | 2.808 | 642.69 |
| 8b | 2.602 | 399.94 |
| 9a | 1.995 | 98.86 |
| Diclofenac sodium | 2.398 | 250 (Exp. LD ₅₀) |
| Ibuprofen | 2.803 | 639 (Exp. LD ₅₀) |

the Cliv-M based pharmacophore and its derivatives that were predicted to be active anti-inflammatory compounds through QSAR and docking studies. Cliv-M derivatives has been designed by side chain modification in the parent skeleton with various halogenating groups and an ester group.

3.3. Molecular docking revealed binding affinity against selected targets

The aim of the molecular docking study was to elucidate whether Cliv-M derivatives modulate the target, and to study their possible mechanisms of action. The results of the molecular docking suggest that derived compounds inhibit the activity of IL6, TNF- α and IL1- β (Sharma et al., 2010; Yadav et al., 2010, 2011; Meena et al., 2011). In the work presented here, we explored the orientations and binding affinities (in terms of the docking energy in kcal mol⁻¹) of Cliv-M derivatives (6a–9a) towards anti-inflammatory and immunomodulatory targets IL6 (PDB:1N26), TNF- α (PDB:2AZ5) and IL1- β (PDB:3O4O) (Figs. 1–3).

The binding affinity obtained in the docking study allowed the activity of the Cliv-M derivatives (6a–9a), to compare with that of the standard anti-inflammatory drugs (Fig. 4). All of the derivatives showed high binding affinities (low docking energies) for targets. The comparison of how the binding pocket amino acid residues of target interacted with the derivatives showed that

Table 3

Compliance of Cliv-M (6a–9a) derivatives to computational parameters of bioavailability and drug likeness properties.

| Compound | Pharmacokinetic property (ADME) dependent on chemical descriptors | | | | | | | | Rule of 5 violation |
|----------------|--|------------------------------------|----------------------------|-------------------|-----------------------|----------------------|---------------------|-------------------|---------------------|
| | A ^a D ^b M ^c Oral bioavailability: TPSA ^e (Å ²) | AE ^d MW ^f | ADME Log P ^g | AD | | | H-bond acceptor | | |
| | | | | H-bond donor | | Hydroxyl group count | Nitrogen atom count | Oxygen atom count | |
| | | | | Amine group count | Sec-amine group count | | | | |
| Cleomiscosin A | 113.127 | 386.357 | 1.822 | 0 | 0 | 2 | 0 | 8 | 0 |
| Cliv-M | 99.558 | 400.387 | 1.853 | 0 | 0 | 1 | 0 | 8 | 0 |
| 6a | 54.409 | 383.615 | 3.922 | 0 | 0 | 0 | 0 | 4 | 0 |
| 6b | 95.263 | 469.274 | 2.889 | 0 | 0 | 1 | 0 | 8 | 0 |
| 7a | 96.124 | 715.969 | 4.404 | 0 | 0 | 1 | 0 | 8 | 1 |
| 8a | 96.417 | 778.072 | 5.009 | 0 | 0 | 1 | 0 | 8 | 2 |
| 8b | 95.224 | 652.176 | 4.368 | 0 | 0 | 1 | 0 | 8 | 1 |
| 9a | 103.569 | 368.342 | 3.366 | 0 | 0 | 0 | 0 | 7 | 0 |

^a A = absorption.

^b D = distribution.

^c M = metabolism.

^d E = excretion.

^e TPSA = topological polar surface area.

^f MW = molecular weight.

^g Log P = octanol/water partition coefficient.

compounds **6a** and **9a** interacted with conserved hydrophobic amino acid residues. Phenylalanine (Phe, F), tyrosine (Tyr, Y), tryptophan (Trp, W), histidine (His, H), lysine (Lys, K), methionine (Met, M), leucine (Leu, L), isoleucine (Ile, I), valine (Val, V), alanine (Ala, A), threonine (Thr, T) and cysteine (Cys, C) are the conserved amino acid residues of anti-inflammatory targets viz., IL6 (PDB:1N26), TNF- α (PDB:2AZ5) and IL1- β (PDB:3O4O), thus lead to more stability and potency in these cases (Table 1). The docking results for the active derivatives showed that compound **9a** docked onto anti-inflammatory and immuno-modulatory targets IL6, TNF- α and IL1- β with high binding affinity, indicated by low docking energy of $-92.45 \text{ kcal mol}^{-1}$, $-94.992 \text{ kcal mol}^{-1}$ and $-67.462 \text{ kcal mol}^{-1}$ respectively (Figs. 1–3).

In **9a**-IL6 complex (Fig. 1), the chemical nature of binding site amino acid residues within a radius of 4\AA were nucleophilic e.g., Ser-101, Ser-152, Ser-224, basic e.g., Lys-105, Lys-154, acidic e.g., Glu-114, Asp-198, hydrophobic e.g., Val-112, aromatic e.g., Phe-103 and polar amide type e.g., Gln-196. Likewise, in **9a**-TNF- α complex (Fig. 2), the chemical nature of binding site amino acids within 4\AA of docked ligand were hydrophobic e.g., Val-13, Ile-155, basic e.g., His-15, hydrophobic e.g., Leu-36, Leu-57, Leu-120, aromatic e.g., Tyr-59, Tyr-119, nucleophilic e.g., Ser-60, polar amide e.g., Gln-61 and hydrophobic, small e.g., Gly-121. Similarly, **9a**-IL1- β complex (Fig. 3) showed acidic residue e.g., Asp-10, basic residues e.g., Arg-13, Lys-26, hydrophobic residues e.g., Ile-15, Ile-25, Pro-28 and aromatic residues e.g., Phe-30, Phe-107 within 4\AA of docked ligand. On the other hand diclofenac-IL6 complex (Fig. 4) also showed similar type of residues in the binding site pocket (within 4\AA radius) such as polar and nucleophilic residue e.g., Ser-101, aromatic and hydrophobic e.g., Phe-103, polar and basic residues e.g., Lys-105, Lys-154, polar and acidic nature residue e.g., Glu-114, polar and amide residue e.g., Gln-196. All bound compounds showed hydrophobic interactions with anti-inflammatory targets, therefore lead to more stability and potency in these compounds, comparable to diclofenac.

Similarly, compound **6a** docked onto anti-inflammatory and immunomodulatory targets IL6, TNF- α and IL1- β with high binding affinity, indicated by low docking energy of $-81.933 \text{ kcal mol}^{-1}$, $-69.235 \text{ kcal mol}^{-1}$ and $-65.985 \text{ kcal mol}^{-1}$ respectively. On the other hand, the docking results for standard anti-inflammatory drug diclofenac with receptors IL6, TNF- α and IL1- β showed a low docking energy of $-64.141 \text{ kcal mol}^{-1}$, $-76.282 \text{ kcal mol}^{-1}$ and $-62.091 \text{ kcal mol}^{-1}$ respectively. In these complexes, the conserved binding pocket amino acid residues were hydrophobic in nature within a selection radius of 4\AA from bound ligand. Superimposition study also suggests the similar binding site residues for most favorable conformations of active compounds during molecular docking experiments.

3.4. Predicting anti-inflammatory activity with the QSAR model

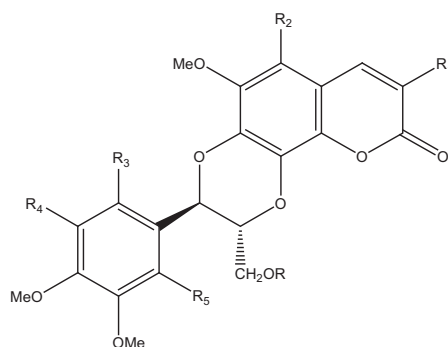
Prior studies related to structure activity relationship of cleomiscosin A methyl ether, showed promising role in the development of anti-inflammatory and immunomodulatory drugs (Sharma et al., 2010). Following so, in the present work, we have predicted the activity of Cliv-M derivatives (**6a–9a**), through QSAR model. The structure–activity relationship denoted by the QSAR model yielded a very high activity–descriptors relationship accuracy of 91.81% referred by regression coefficient ($r^2 = 0.918119$) and a high activity prediction accuracy of 86.73% ($rCV^2 = 0.867314$) (Fig. 5). Seven chemical descriptors were found to be applicable to the activity. The QSAR equation indicated that chemical descriptors namely, dipole vector X, dipole vector Y, steric energy, LUMO energy, size of smallest ring, size of largest ring and carboxyl group count correlated well with activity. The QSAR model equation given below (Eq. (1)), showing the relationship

Table 4
Compliance of active Cliv-M derivatives (**6a–9a**) to computational parameters of pharmacokinetics (ADME).

| Compound name | logS for aqueous solubility | logKhsa for serum protein binding | logBB for brain/blood | No. of metabolic reactions | Predicted CNS activity | logHERG for K ⁺ channel blockage | Apparent Caco-2 Permeability (nm/s) | Apparent MDCK Permeability (nm/s) | logKp for skin permeability | $J_{in,max}$ transdermal transport rate | Jorgensen rule of 3 violations | % Human oral absorption in GI ($\pm 20\%$) | Qual. model for human oral absorption |
|---------------------------|-----------------------------|-----------------------------------|-----------------------|----------------------------|--------------------------------|---|-------------------------------------|-----------------------------------|----------------------------------|---|--------------------------------|--|---------------------------------------|
| Cleomiscosin A | -4.355 | -0.078 | -1.41 | 5 | -2 | -5.69 | 266.413 | 118.425 | -3.26 | 0.009 | 0 | 82.308 | High |
| Cliv-M | -4.823 | 0.045 | -1.082 | 5 | -2 | -5.79 | 587.266 | 278.284 | -2.655 | 0.013 | 0 | 92.525 | High |
| 6a | -5.574 | 0.388 | 0.39 | 2 | 1 | -5.265 | 2328.76 | 10,000 | -1.815 | 0.016 | 0 | 100 | High |
| 6b | -5.669 | 0.209 | -0.802 | 5 | -1 | -5.439 | 584.821 | 1124.282 | -2.884 | 0.001 | 0 | 96.806 | High |
| 7a | -6.996 | 0.472 | -0.424 | 5 | -1 | -5.221 | 665.586 | 7223.035 | -3.004 | 0 | 1 | 91.346 | Low |
| 8a | -6.987 | 0.457 | -0.488 | 5 | -1 | -5.413 | 683.184 | 5639.442 | -2.923 | 0 | 1 | 91.052 | Low |
| 8a | -6.078 | 0.298 | -0.761 | 5 | -1 | -5.513 | 585.003 | 1517.212 | -2.893 | 0.001 | 1 | 85.612 | High |
| 9a | -5.43 | 0.219 | -1.283 | 2 | -2 | -6.749 | 302.253 | 135.735 | -2.979 | 0.001 | 0 | 89.448 | High |
| Diclofenac sodium | -5.176 | -0.032 | -0.05 | 4 | -1 | -2.547 | 483.646 | 1001.69 | -1.589 | 2.140 | 0 | 100 | High |
| Stand. range ^a | (-6.5/0.5) | (-1.5/1.5) | (-3.0/1.2) | (1.0/8.0) | -2 (inactive) +2 active) | (concern below -5) | (<25 poor, >500 great) | (<25 poor, >500 great) | (-8.0 to -1.0, Kp in cm/h) | ($\mu\text{g}/\text{cm}^2 \text{ h}$) | (maximum is 3) | (<25% is poor) (>80% is high) | |

^a For 95% of known drugs based on Schrodinger, USA – Qikprop v3.2 (2009) software results.

Table 7
% Inhibition of pro-inflammatory cytokines of derivatives **6a–9a**.



6a: R₁ = R₂ = R₅ = Cl; R = R₃ = R₄ = H
6b: R₂ = R₃ = Cl; R = R₁ = R₄ = R₅ = H
7a: R₁ = R₂ = R₃ = R₄ = Br; R = R₅ = H
8a: R₁ = R₂ = R₄ = I; R = R₃ = R₅ = H
8b: R₂ = R₃ = I; R = R₄ = R₅ = H
9a: R = -COOCH₃; R₁ = R₂ = R₃ = R₄ = R₅ = H

| Compound | R ₁ | R ₂ | R ₃ | R ₄ | R ₅ | R | Dose (μg/ml) | % inhibition of Pro-inflammatory cytokines | | |
|-------------------|----------------|----------------|----------------|----------------|----------------|---------------------|--------------|--|----------------------------|-----------------------------|
| | | | | | | | | TNF-α (Mean ± SE) | IL-1β (Mean ± SE) | IL-6 (Mean ± SE) |
| Vehicle (DMSO) | - | - | - | - | - | - | - | 0.00 ± 0.00 | 0.00 ± 0.00 | 0.00 ± 0.00 |
| 6a | -Cl | -Cl | -H | -H | -Cl | -H | 1 | 14.14 ± 6.79 ^{ns} | 24.46 ± 7.26 ^{ns} | 9.07 ± 7.36 [*] |
| | | | | | | | 10 | 20.63 ± 5.01 [*] | 28.98 ± 2.88 [*] | 21.92 ± 6.40 [*] |
| 6b | -H | -Cl | -Cl | -H | -H | -H | 1 | 11.96 ± 8.04 ^{ns} | 24.90 ± 4.67 ^{ns} | 27.67 ± 22.97 [*] |
| | | | | | | | 10 | 19.16 ± 6.32 [*] | 30.77 ± 5.45 ^{**} | 17.45 ± 4.98 ^{ns} |
| 7a | -Br | -Br | -Br | -Br | -H | -H | 1 | 13.42 ± 9.80 ^{ns} | 24.64 ± 8.52 ^{ns} | 16.78 ± 9.38 ^{ns} |
| | | | | | | | 10 | 14.80 ± 10.02 ^{ns} | 28.56 ± 6.42 [*] | 28.88 ± 16.46 ^{ns} |
| 8a | -I | -I | -H | -I | -H | -H | 1 | 11.15 ± 12.39 ^{ns} | 28.13 ± 5.27 [*] | 23.46 ± 16.46 [*] |
| | | | | | | | 10 | 22.51 ± 6.11 ^{**} | 31.79 ± 6.42 ^{**} | 23.60 ± 17.32 ^{ns} |
| 8b | -H | -I | -I | -H | -H | -H | 1 | 13.28 ± 10.46 ^{ns} | 31.21 ± 7.79 ^{**} | 6.95 ± 6.46 [*] |
| | | | | | | | 10 | 23.46 ± 5.21 ^{**} | 34.60 ± 8.45 | 13.06 ± 7.73 ^{ns} |
| 9a | -H | -H | -H | -H | -H | -COOCH ₃ | 1 | 11.79 ± 9.70 ^{ns} | 26.44 ± 7.75 [*] | 16.64 ± 17.82 [*] |
| | | | | | | | 10 | 17.68 ± 7.07 ^{ns} | 27.73 ± 8.68 [*] | 23.28 ± 18.58 [*] |
| Diclofenac Sodium | - | - | - | - | - | - | 1 | 27.56 ± 6.10 ^{**} | 36.47 ± 9.57 ^{**} | 30.99 ± 20.40 ^{ns} |
| | | | | | | | 10 | 29.78 ± 9.34 ^{**} | 40.49 ± 6.72 ^{**} | 43.16 ± 16.71 ^{**} |

Vehicle vs treatment; ns – not significant; n = 6.

* P < 0.05.

** P < 0.001.

between experimental activity *in vivo* [i.e., the lethal dose to 50% of the population (LD₅₀)] as the dependent variable and seven independent variables i.e., chemical descriptors:

$$\begin{aligned} \text{Predicted log LD}_{50} (\text{mg/kg}) = & +0.207651 \times \text{dipole vector X (debye)} \\ & -0.0872917 \times \text{dipole vector Y (debye)} \\ & +0.0150386 \times \text{steric energy (kcal/mole)} \\ & +0.102653 \times \text{LUMO energy (eV)} \\ & +1.26128 \times \text{size of smallest ring} \\ & +0.563956 \times \text{size of largest ring} \\ & -0.724896 \times \text{group count (carboxyl)} \\ & -7.41586 \end{aligned} \quad (1)$$

Here, rCV² (the cross-validation regression coefficient) = 0.867314, which indicates that the newly derived QSAR model has a prediction accuracy of 86.73%, and r² (regression coefficient) = 0.918119, which indicates that the correlation between the activity (dependent variable) and the descriptors (independent variables) for the training data set compounds was 91.81%. Thus, we successfully developed a predictive QSAR model for *in vivo* anti-inflammatory activity of Cliv-M derivatives (**6a–9a**). A multiple linear regression QSAR model was developed for activity prediction that successfully and accurately (noting the corresponding experimental activities) predicted the activities of newly

designed Cliv-M derivatives (**6a–9a**) that had the basic pharmacophore. The QSAR model quantified the activity-dependent chemical descriptors and predicted the LD₅₀ of each derivative, thus indicating its potential range of effective dose (ED₅₀) (Table 2, Fig. 5). Results showed that the predicted activities were comparable with those obtained experimentally. Compound **9a** has higher activity, while compound **6a** showed comparable activity than diclofenac sodium.

3.5. Assessment through pharmacokinetic parameters

We considered several physicochemical properties related to pharmacokinetics, when screening for active derivatives. The results revealed that all of the derivatives followed Lipinski's rule of five (Table 3). The hydrophilicity of each compound measured through its logP value. Low hydrophilicity and therefore a high logP value may lead to poor absorption or permeation. For compounds to have a reasonable probability of being well absorbed, it has found that their logP values must not be >5. All compounds showed calculated logP values less than 5, so these will be soluble in aqueous solution and hence able to gain access to membrane surfaces. Lipophilicity (ratio of a molecule's solubility in octanol to solubility in water) measured through logP. logP value linked to blood–brain barrier penetration and utilized to predict permeability. The process of excretion, which eliminates the compound

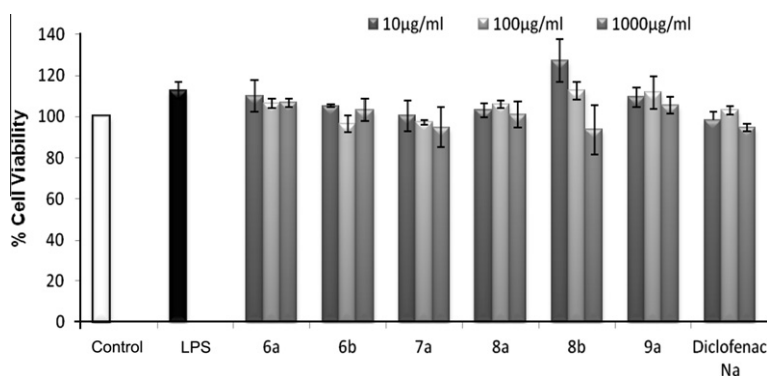


Fig. 6. % Cell viability of compounds (6a–9a) using MTT assay.

from the human body, depends on its molecular weight and log P (Yadav et al., 2011). Molecules with intermediate lipophilicities have a better chance of arriving at the receptor site (Yadav et al., 2011; Hodgson, 2001; Sean et al., 2006; Norinder and Bergström, 2006). Similarly, all compounds showed calculated molecular weight less than 500 Da, making these likely to have high solubility and to pass through cell membranes easily. All the derivatives have polarities that enabled better permeation and absorption, as revealed by the number of H-bond donors and H-bond acceptors.

Similarly, the ADME parameters calculated for the active derivatives and the values of these parameters showed close correspondence with those of standard drugs and fell within the standard range of values exhibited by 95% of all known drugs. Typically, low solubility is associated with bad absorption, so the general aim is to avoid poorly soluble compounds. The aqueous solubility (log S) of a compound significantly affects its absorption and distribution characteristics. The calculated log S values of the studied compounds were within the acceptable interval. Calculations related to solubility, serum protein binding, the blood–brain barrier (log BB and apparent MDCK cell permeability), gut–blood barrier (Caco-2 cell permeability), central nervous system activity, metabolic reactions, log IC_{50} for hERG K⁺ channel blockage, skin permeability (K_p) and human oral absorption in the gastrointestinal tract showed that the values for the active derivatives fall within the standard ranges generally observed for the drugs (Table 4).

3.6. Toxicity risk assessment

In the present study, we calculated toxicity risk parameters for example, mutagenicity, tumorigenicity, irritation, and reproductive/developmental toxicities of the Cliv-M derivatives. The toxicity risk predictor locates fragments within a molecule that indicate a potential toxicity risk. Toxicity screening results showed that none of the compounds presented a risk of reproductive or developmental toxicity. To judge the compound's overall potential to act as a drug, we calculated its overall drug score, which combines its drug likeness and toxicity risk parameter values. The calculated parameters of drug likeness for the active compounds were within the acceptable interval, if used in long term, similar to standard drugs (Table 5). Results revealed that the overall drug scores of active compounds are comparable to that of standard drugs.

3.7. *In vitro* anti-inflammatory activity

Inflammation is the body's immediate response to damage to its tissues and cells by pathogens, noxious stimuli such as chemicals, or physical injury. Acute inflammation is a short-term response that usually results in healing: leukocytes infiltrate the damaged region, removing the stimulus and repairing the tissue. Chronic inflammation, by contrast, is a prolonged, dysregulated and mal-

adaptive response that involves active inflammation, tissue destruction and attempts at tissue repair. Such persistent inflammation is associated with many chronic inflammatory conditions, including allergy, atherosclerosis, cancer, arthritis and autoimmune diseases. The target based anti-inflammatory activities of compounds 6a–9a (Tables 6 and 7) have been evaluated in *in vitro* condition at the initial dose of 1 µg / ml and 10 µg / ml. When compared with the standard drug Diclofenac sodium it was seen that the compounds 6a, 7a, 8b and 9a showed significant inhibition of pro-inflammatory targets in lipo-polysaccharide (LPS) induced inflammation in primary macrophages cell culture model. The pro-inflammatory cytokines (IL-1 β , IL-6 and TNF- α) quantified from cell culture supernatant using enzyme linked immunosorbent assay (ELISA). The compounds 6a, 7a, 8b and 9a showed the significant inhibition of pro-inflammatory targets, which are the mediators of various chronic inflammatory disorders. The *in vitro* effect of 6a–9a on cell viability in mouse peritoneal macrophage cells isolated from mice was evaluated using MTT assay. The significant change in percent cell population was not observed ($P < 0.05$) at any concentration of the treatment when compared with normal cells. The % cell viability MTT assay of all the synthesized compounds was carried out and the results were shown in Fig. 6.

4. Conclusion

In conclusion, we report the polyhalogenation reactions of cliv A methyl ether using a modified method of Surya Prakash et al. When Cliv-M was treated with $BF_3 \cdot Et_2O$ and NXS ($X = Cl, Br$ and I) at room temperature, we obtained a series of polyhalogenated compounds like trichloro, dichloro, tetrabromo, triiodo and diiodo derivatives (6a–8a). An ester derivative, 9a was also formed when Cliv-M was refluxed with potassium carbonate, dimethyl carbonate and DMF. All the above derivatives 6a–9a were made for the first time from cleomiscosin A methyl ether. In addition, the synthesized derivatives were tested for *in vitro* target based anti-inflammatory activity. The preliminary *in vitro* studies on these derivatives concluded that compound 6a, 7a, 8b and 9a showed the significant inhibition of pro-inflammatory targets, which are the mediators of various chronic inflammatory disorders. These findings suggested that compounds 6a and 9a inhibit ($P < 0.05$) the production of TNF- α , IL-1 β and IL-6 at concentration level of 10 µg/ml. The production of TNF- α was significantly inhibited by compounds 6b and 7a at concentration of 10 and 1 µg/ml, similarly IL-1 β was inhibited by 6a, 7a, 8a and 9a at concentration level of 1 and 10 µg/ml. Molecular docking and QSAR studies was also performed on Cliv-M derivatives (6a–9a) in order to predict the potential anti-inflammatory compounds. During the molecular docking studies, all of the derivatives showed high binding affinities against selected anti-inflammatory targets. Linear model is developed by the forward stepwise multiple linear regression method to link

the structures to their reported activity. The QSAR study indicates that chemical descriptors are well correlated with anti-inflammatory activity. Based on oral bioavailability, drug likeness, ADMET and toxicity risk assessments studies, we concluded that compound **9a** possesses higher activity than diclofenac sodium, while compound **6a** showed comparable activity than diclofenac. The calculated parameters of drug likeness and ADME for the active compounds were within the acceptable interval. Results indicated no sign of toxicity, similar to standard drug diclofenac. Results also revealed that the overall drug scores of active compounds are comparable to that of standard drugs.

Acknowledgements

The authors are grateful to the Director, CIMAP (CSIR), Lucknow for providing necessary facilities and encouragement. One of the author (Shelly Sharma) is grateful to DST (Department of Science and Technology) for their financial support. The Communication number of this manuscript is 2012–110J.

Appendix A. Supplementary material

Supplementary data associated with this article can be found, in the online version, at <http://dx.doi.org/10.1016/j.ejps.2012.09.008>.

References

- Bawankule, D.U., Chattopadhyay, S.K., Pal, A., Saxena, K., Yadav, S., Faridi, U., Darokar, M.P., Gupta, A.K., Khanuja, S.P.S., 2008. Modulation of inflammatory mediators by coumarino-lignoids from *Cleome viscosa* in female swiss albino mice. *Inflammopharmacology* 16, 272–277.
- Brown, E., Yedjou, C.G., Tchounwou, P.B., 2008. Cytotoxicity and oxidative stress in human liver carcinoma cells exposed to arsenic trioxide (HepG2). *Met. Ions Biol. Med.* 10, 583–587.
- Butler, M.S., 2008. Natural products to drugs: natural product-derived compounds in clinical trials. *Nat. Prod. Rep.* 25, 475–516.
- Chattopadhyay, S.K., Thakur, R.S., Patnaik, G.K., Srimal, R.C. Indian Patent No. 182638, Date of grant 17-12-1999.
- Chin, Y.W., Balunas, M.J., Chai, H.B., Kinghorn, A.D., 2006. Drug discovery from natural sources. *AAPS J.* 8, 239–253.
- Clark, D.E., 1999. Rapid calculation of polar molecular surface area and its application to the prediction of transport phenomena. 1. Prediction of intestinal absorption. *J. Pharm. Sci.* 88, 807–814.
- Ertl, P., Rohde, B., Selzer, P., 2000. Fast calculation of molecular polar surface area as a sum of fragment based contributions and its application to the prediction of drug transport properties. *J. Med. Chem.* 43, 3714–3717.
- Gautam, R., Jachak, S.M., 2009. Recent developments in anti-inflammatory natural products. *Med. Res. Rev.* 29, 767–820.
- Hodgson, J., 2001. ADMET-turning chemicals into drugs. *Nat. Biotechnol.* 19, 722–726.
- Jung, H.W., Yoon, C.H., Kim, Y.H., Boo, Y.C., Park, K.M., Park, Y.K., 2007. Wen-Pi-Tang-Hab-Wu-Ling-San extracts inhibits the release of inflammatory mediators from LPS – stimulated mouse macrophages. *J. Ethnopharmacol.* 114, 439–445.
- Lipinski, C.A., Lombardo, F., Dominy, B.M., Feeney, P., 2001. Experimental and computational approaches to estimate solubility and permeability in drug discovery and development settings. *Adv. Drug Deliv. Rev.* 46, 3–26.
- Lombardo, F., Gifford, E., Shalaeva, M.Y., 2003. *In silico* ADME prediction: data, models, facts and myths. *Mini-Rev. Med. Chem.* 3, 861–875.
- Martin, C., 1999. A general and fast scoring function for protein ligand interactions: a simplified potential approach. *J. Med. Chem.* 42, 791–804.
- Meena, A., Yadav, D.K., Srivastava, A., Khan, F., Chanda, D., Chattopadhyay, S.K., 2011. *In silico* exploration of anti-inflammatory activity of natural coumarinolignoids. *Chem. Biol. Drug Des.* 78, 567–579.
- Minagar, A., Shapshak, P., Fujimura, R., Ownby, R., Heyes, M., Eisdorfer, C., 2002. The role of macrophage/microglia and astrocytes in the pathogenesis of three neurologic disorders: HIV-associated dementia, Alzheimer disease, and multiple sclerosis. *J. Neurol. Sci.* 202, 13–23.
- Muegge, I., 2000. A knowledge-based scoring function for protein–ligand interactions: probing the reference state. *Perspec. Drug Dis. Des.* 20, 99–114.
- Norinder, U., Bergström, C.A.S., 2006. Prediction of ADMET properties. *Chem. Med. Chem.* 1, 920–937.
- Olah, G.A., 1993. Superlectrophiles. *Angew. Chem., Int. Ed. Engl.* 32, 767–788.
- Olah, G.A., Prakash, G.K.S., Lammerstma, K., 1989. Protonated (protosolvated) onium ions (onlum dications). *Res. Chem. Intermed.* 12, 141–159.
- Olah, G.A., Mathew, T., Marinez, E.R., Esteves, P.M., Etkorn, M., Rasul, G., Prakash, G.K.S., 2001. Acid-catalyzed isomerization of Pivalaldehyde to methyl isopropyl ketone via a reactive protosolvated carboxonium ion intermediate. *J. Am. Chem. Soc.* 123, 11556–11561.
- Ray, A.B., Chattopadhyay, S.K., Kumar, S., Konno, C., Kisso, Y., Hikino, H., 1985. Structures of cleomiscosins, coumarinolignoids of *Cleome viscosa* seeds. *Tetrahedron* 41, 209–214.
- Reichel, A., Begley, D., 1998. Potential of immobilized artificial membranes for predicting drug penetration across the blood–brain barrier. *Pharm. Res.* 15, 1270–1274.
- Sean, E., Sergey, A., Andy, R., Eugene, K., Eugene, A., Rakhmatulin, S.S., Bugrim, A., Nikolskaya, T., 2006. A combined approach to drug metabolism and toxicity assessment. *Drug Metab. Dispos.* 34, 495–503.
- Sharma, S., Chattopadhyay, S.K., Trivedi, P., Bawankule, D.U., 2010. Synthesis and anti-inflammatory activity of derivatives of coumarino-lignoid, cleomiscosin A and its methyl ether. *Eur. J. Med. Chem.* 45, 5150–5156.
- Surya Prakash, G.K., Mathew, T., Hoole, D., Esteves, P.M., Wang, Q., Rasul, G., Olah, G.A., 2004. N-Halosuccinimide/BF₃–H₂O, efficient electrophilic halogenating systems for aromatics. *J. Am. Chem. Soc.* 126, 15770–15776.
- The Wealth of India (Raw Materials), 1950. CSIR, New Delhi, 2C, p. 231.
- Veber, D.F., Stephen, R., Johnson, H.Y., Cheng, B.R., Smith, W., Kopple, K.D., 2002. Molecular properties that influence the oral bioavailability of drug candidates. *J. Med. Chem.* 45, 2615–2623.
- Yadav, D.K., Meena, A., Srivastava, A., Chanda, D., Khan, F., Chattopadhyay, S.K., 2010. Development of QSAR model for immunomodulatory activity of natural coumarino-lignoids. *Drug Des. Dev. Ther.* 4, 173–186.
- Yadav, D.K., Khan, F., Negi, A.S., 2011. Pharmacophore modeling, molecular docking, QSAR, and *in silico* ADMET studies of gallic acid derivatives for immunomodulatory activity. *J. Mol. Model.* <http://dx.doi.org/10.1007/s00894-011-1265-3>.